Solar Panels for the Lunar Base

Leulaye Maskal[a,b], Christian Singleton[a], Ahmed Aboudiwan[c], Ali Taha[d], Malgorzata Marciniak[*a]
[a]LaGuardia Community College of CUNY, Department of Mathematics, Engineering, and Computer Science, 31-10 Thomson Avenue, Long Island City, NY 11101; [b]NASA-GISS, 2880 Broadway, New York, NY 10025; [c]College of Staten Island of CUNY, 2800 Victory Blvd, Staten Island, NY, 10314; [d]Cornell University, College of Engineering, Carpenter Hall, 313 Campus Rd, Ithaca, NY 14853

ABSTRACT

The motivation behind this research lies in the well-spread news about USA and China's plans to build bases on the moon within the next 10 years. In this research, we create a mathematical model of efficiency for geometrical solar panels, as well as discuss which locations on the moon may be suitable for placing a non-tracing solar power plant. We consider the North Pole, the Equator and additional locations; and analyze the accumulation of illumination over an 18.6-year period that represents the lunar cycle. The simulation for geometrical panels is based on the etendue, with the panel being the diaphragm and a selected segment of the sky being the source. However, the etendue needs to be modified due to the properties of solar energy. The selected segment of the sky is crafted with careful analysis of the motion of the moon. The difficulty of the model comes from the fact that the motion of the sun on the moon's sky is subject to change in its speed and direction, which is created by the moon's libration. In addition, we discuss the change of luminosity of the sun's light due to the varied distance between the moon and the sun. The simulation was performed using MATLAB and Mathematica.

Keywords: geometrical shapes of solar panels, mathematical simulation, efficiency of solar panels, lunar base

1. INTRODUCTION

The current exposition is a continuation of our long-term efforts to build reliable mathematical models that express the efficiency of geometrical (shaped) non-tracking solar panels, described in [3], [4], and [5]. The model takes into the consideration the motion of the sun on the sky. The motivation behind the choice of the location lies in the well-spread news of USA and China's plans to build a base on the moon within the next decade, as well as new evidence of ice (H20) on the moon. This evidence was collected from an official NASA press release [8]. In previous expositions we used modified mathematical flux to express the efficiency of geometrical solar panels on Earth and other locations. This approach is not suitable for the lunar base since the trajectory of the Moon is much more complicated than the trajectory of the Earth. The motion of the sun on the moon's sky is subject to change in its speed and direction, which is created by the moon's libration, as described in [2]. Thus, in this research, we create a mathematical model of efficiency for geometrical solar panels based on the etendue with the panel being the diaphragm and a selected segment of the sky being the source. The selected segment of the sky is crafted with analysis of the motion of the moon. A part of building the model of efficiency, is understanding the elliptical orbit of the Moon around the Sun, the Moon's ecliptic path, the latitudinal and longitudinal libration of the Moon, and the Moon's rotation about its axis. Efficiency is a holistic and cumulative value; it considers all potential variations of the moons orbit during its full lunar period. This broad consideration gives us insight into the productivity of differing geometrical panels over a longer period. We analyze the luminosity on the moon to show that the difference between the perihelion and the aphelion on the moon's elliptic path can be omitted in our model. Luminosity also gives us a quantitative understanding of how much energy a solar panel at the lunar base can collect. At the selected locations, the efficiency of each of the solar panel shapes are calculated with software, MATLAB and Mathematica.

*goga@mimuw.edu.pl; phone 1 573 462 0411

2. THE SUN & MOON

2.1 The path of the Sun on the Moons sky

A new mathematical model is required to approximate the efficiency of geometrical solar panels for a lunar base, due to the Moon's complex motion. This motion affects the trajectory of the Sun on the Moon's sky. This section contains astronomical information necessary for understanding the motivation and preparation of the model.
As it was mentioned before, the Moon experiences a latitudinal libration, which is a nodding motion in the vertical direction, and, as indicated in [2], has a maximum change of 6.87º. The Moon also is a subject to a tilt of 1.5º off its axis in the vertical direction. This tilt value is pulled from a report *The Lunar Orbit Throughout Time and Space* [1]. The Sun's disk has a diameter of 0.5º, found in NASA lunar fact sheet titled *Lunar Constants and Models* [6]. Due to libration, the trajectory of the Sun on the Moon's sky has a sinusoidal shape. When adjusting the model for these factors and tracing the path of the Sun on the sky of the Moon, we will use the value: $6.87° + 1.5° + 0.5° = 8.87° \approx 0.154811\ rad$. In our model, the number 8.87º represents the maximum amplitude of the sinusoidal shape. The value of 8.87º influences the ranges of the parameter ϕ in the model. However, the exact ranges vary, depending on the location of the panels on the Moon.
When considering the path of the Sun on the sky at the Moon's North Pole, the sinusoidal trace is observed along the horizon, with the previously mentioned maximum amplitude of 8.87º representing the vertical change of the Sun's rise in the sky. The North Pole receives the sunlight all the time, but only when the amplitude of the sinusoidal shape has a positive value. A negative value represents the Sun dipping below the horizon, which prevents the solar panel from receiving the sunlight. Because the North Pole receives sunlight as the sun makes a full circle, we can represent this range with parameter θ between 0 to 2π. A sketch of the light source on the North Pole is presented on Figure 1.

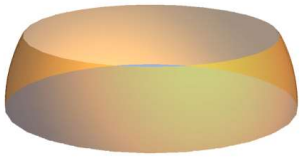

Figure 1. The North Pole. A sketch of the light source used in the etendue

When considering the path of the Sun on the Equator of the Moon, the sinusoidal trace occurs along the vertical direction is visualized as a semicircle above the observer. The amplitude represents a horizontal change in the path of the Sun in the sky. A solar panel at the Equator will only receive sunlight for roughly half of a lunar day, but, unlike the North Pole, there will never be a time the Sun disappears from observer's view during lunar day, so the entire amplitude is considered. The range of the parameter θ in the calculations in the Equator spans from 0 to π because the panel only receives sunlight for half of a lunar day, representing half of a circular rotation. The entire amplitude represented by the parameter ϕ spans between -8.87 º to +8.87 º, i.e., to the right and to the left of the vertical semicircle above the observer. A sketch of the light source at the Equator is presented on Figure 2.

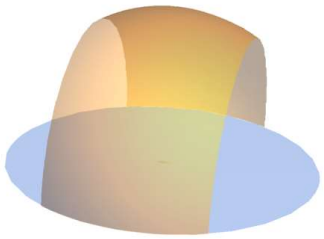

Figure 2. Equator. A sketch of the light source used in the etendue.

A full lunar period is known to be equal to 18.6 (Earth) years, as mentioned in [2]. In our model we assume that over the full lunar period, a summation of each sinusoidal curve created by the Sun's path on the Moon's sky per lunar day, is represented by a spherical segment and parameterized by:

$$\vec{S}(\theta,\phi) = \langle \cos\theta \sin\phi\,, \sin\theta \sin\phi\,, \cos\phi \rangle. \quad (1)$$

The coordinate system is in this model is chosen the same way as in the previous models, described for example in [3]. The spherical segment represents the part of the sky where the sun will travel. This spherical segment is said to have a width represented by the maximum and minimum amplitude of ϕ. Thus, the parameters θ and ϕ have the following ranges:

$$\text{On the North Pole: } \theta \in [0,2\pi] \text{ and } \phi \in \left[\frac{\pi}{2} - 0.15, \frac{\pi}{2}\right] \quad (2)$$

$$\text{On the Equator: } \theta \in [-\frac{\pi}{2}, \frac{\pi}{2}] \text{ and } \phi \in \left[\frac{\pi}{2} - 0.15, \frac{\pi}{2} + 0.15\right] \quad (3)$$

For the future calculations of the etendue, the normal vector is needed. It is calculated as the cross product of the tangent vectors:

$$\frac{\partial \vec{S}}{\partial \phi} = \langle \cos\theta \cos\phi\,, \sin\theta \cos\phi\,, -\sin\phi \rangle \quad (4)$$

$$\frac{\partial \vec{S}}{\partial \theta} = \langle -\sin\theta \sin\phi\,, \cos\theta \sin\phi\,, 0 \rangle \quad (5)$$

Thus,

$$\vec{N} = \frac{\partial \vec{S}}{\partial \theta} \times \frac{\partial \vec{S}}{\partial \phi} = \langle \cos\theta \sin^2\phi\,, \sin\theta \sin^2\phi\,, \cos\phi \sin\phi \rangle. \quad (6)$$

2.2 Etendue and efficiency

Etendue quantifies the relationship between a light source (surface S parameterized by $\vec{S}(\theta,\phi)$ with normal vector $\vec{N}$) and a light collector (diaphragm, surface *r* parameterized by $\vec{r}(x,y)$ with normal vector $\vec{n}$) . To be precise, the etendue measures the agreement between the directions of the normal vectors ($\vec{N}$ and $\vec{n}$) from the two surfaces and is defined as a double surface integral of the dot product between two normal vectors:

$$Etendue = \iint_S \iint_r \vec{N} \cdot \vec{n}\, d\vec{r} \cdot d\vec{S} \quad (7)$$

In this model the integration is performed only for the range of the parameters, where $\vec{N} \cdot \vec{n} > 0$. Calculating along the ranges of the parameters, where $\vec{N} \cdot \vec{n} < 0$ would indicate that the panel is losing energy when the sunlight shines on the non- photovoltaic side of the panel, which does not take place.
In our model the solar panel is the diaphragm and a selected segment of the sky is the light source. Efficiency is a unit-less value and its meaning is defined through comparison among the obtained results. A single value of efficiency for a panel is virtually useless, but with a collection of calculated efficiencies we can compare and contrast using ratio analysis. The efficiency of the shape is defined as the ratio of the etendue and the surface area of the panel.

2.3 Luminosity

To analyze the intensity of the light source we use the concept of luminosity, which is a measure of the amount of power a source releases, and flux is the measure of power per square area an object will receive. Aphelion is the location on the Moon's orbit with the furthest distance from the Sun, and the perihelion is the location of the closest distance. The values for the distances were found in a NASA planetary fact sheet [9]. Flux is determined by both the distance from the power source an object is and the amount of power the source releases. The formula for calculating flux is:

$$Flux = \frac{Luminosity}{4\pi \times (distance)^2} \text{ W/m}^2 \quad (8)$$

Using the value of solar luminosity of $3.826 \times 10^{26} W$ we calculate the flux at the perihelion as

$$\frac{3.826\times10^{26}}{4\pi\times(147090000000)^2} = 1{,}407.24 \text{ W/m}^2 \tag{9}$$

And the flux at the aphelion as

$$\frac{3.826\times10^{26}}{4\pi\times(152100000000)^2} = 1{,}316.06 \text{ W/m}^2. \tag{10}$$

This shows that the variability of the flux received by the Moon is in the range of:

$$\frac{1{,}407.24-1{,}316.06}{1{,}407.24} = \frac{91.18}{1{,}407.24} \approx 6.48\% \tag{11}$$

Thus, the variability of the flux caused by varied distance from the Sun will be omitted in the current model.

3. CALCULATIONS AT THE NORTH POLE

As mentioned before, the surface of the spherical segment of the light source is parameterized by the following equation:

$$\vec{S}(\theta,\phi) = \langle \cos\theta \sin\phi\, , \sin\theta \sin\phi\, , \cos\phi \rangle \tag{12}$$

with the range of the parameters $\theta \in [0,2\pi]$ and $\phi \in \left[\frac{\pi}{2} - 0.15, \frac{\pi}{2}\right]$. The normal vector is calculated as

$$\vec{N} = \langle \cos\theta \sin^2\phi\, , \sin\theta \sin^2\phi\, , \cos\phi \sin\phi \rangle. \tag{13}$$

Most parametrizations are identical to those in [3].

3.1 Horizontal Panel

The surface of a flat horizontal panel is parametrized by the equation $\vec{r}(x,y) = \langle x, y, 0\rangle$, with the range of the parameters $x \in [0,1]$ and $y \in [0,1]$. Its area is 1. Then the tangent vectors are

$$\frac{\partial\vec{r}}{\partial x} = \langle 1,0,0\rangle \text{ and } \frac{\partial\vec{r}}{\partial y} = \langle 0,1,0\rangle \tag{14}$$

And the normal vector is

$$\vec{n} = \frac{\partial\vec{r}}{\partial x} \times \frac{\partial\vec{r}}{\partial y} = \langle 0,0,1\rangle \tag{15}$$

The dot product of $\vec{N}$ and $\vec{n}$ is

$$\vec{N} \cdot \vec{n} = \langle \cos\theta \sin^2\phi\, , \sin\theta \sin^2\phi\, , \cos\phi \sin\phi \rangle \cdot \langle 0,0,1\rangle = \cos\phi \sin\phi \tag{16}$$

A quadruple integral that expresses the efficiency is calculates as follows but only these parameters, where $\vec{N} \cdot \vec{n} > 0$. The surface integrals are calculated as in [7].

$$\iint_S \iint_r \vec{N} \cdot \vec{n}\, d\vec{r} \cdot d\vec{S} = \int_0^1 \int_0^1 \int_0^{2\pi} \int_{1.415}^{\frac{\pi}{2}} \cos\phi \sin\phi \; d\phi\, d\theta\, dx\, dy = 0.0747 \tag{17}$$

3.2 Vertical Panel

The surface of the flat vertical panel is parametrized by the equation $\vec{r}(y,z) = \langle 0, y, z\rangle$, with the range of the parameters $y \in [0,1]$ and $z \in [0,1]$. Its area is 1. Then the tangent vectors are

$$\frac{\partial \vec{r}}{\partial z} = \langle 0,0,1\rangle \text{ and } \frac{\partial \vec{r}}{\partial y} = \langle 0,1,0\rangle \tag{18}$$

And the normal vector is

$$\vec{n} = \frac{\partial \vec{r}}{\partial z} \times \frac{\partial \vec{r}}{\partial y} = \langle 1,0,0\rangle \tag{19}$$

The dot product of $\vec{N}$ and $\vec{n}$ is

$$\vec{N} \cdot \vec{n} = \langle \cos\theta \sin^2\phi\,, \sin\theta \sin^2\phi\,, \cos\phi \sin\phi\rangle \cdot \langle 1,0,0\rangle = \cos\theta \sin^2\phi \tag{20}$$

A quadruple integral that expresses the efficiency is calculates as follows but only these parameters, where $\vec{N} \cdot \vec{n} > 0$:

$$\iint_S \iint_r \vec{N} \cdot \vec{n}\, d\vec{r} \cdot d\vec{S} = \int_0^1 \int_0^1 \int_0^{2\pi} \int_{1.415}^{\frac{\pi}{2}} \cos\theta \sin^2\phi \; d\phi\, d\theta\, dx\, dy = 0.307 \tag{21}$$

3.3 Cylindrical Panel

The surface of the cylindrical panel, with radius 1 and height 1 is parametrized by the equation $\vec{r}(u,v) = \langle \sin u\,, \cos u\,, -v\rangle$. The range of parameters is $u \in \left[\frac{-\pi}{2}, \frac{3\pi}{2}\right]$ and $v \in [-1,0]$ and its area is 2π. Then the tangent vectors are

$$\frac{\partial \vec{r}}{\partial u} = \langle \cos u\,, -\sin u\,, 0\rangle \text{ and } \frac{\partial \vec{r}}{\partial v} = \langle 0,0,-1\rangle \tag{22}$$

With the normal vector

$$\vec{n} = \frac{\partial \vec{r}}{\partial u} \times \frac{\partial \vec{r}}{\partial v} = \langle \sin u\,, \cos u\; 0\rangle \tag{23}$$

The dot product of $\vec{N}$ and $\vec{n}$ is

$$\vec{N} \cdot \vec{n} = \langle \cos\theta \sin^2\phi\,, \sin\theta \sin^2\phi\,, \cos\phi \sin\phi\rangle \cdot \langle \sin u\,, \cos u, 0\rangle = \cos\theta \sin u \sin^2\phi + \sin\theta \cos u \sin^2\phi \tag{24}$$

which simplifies to

$$\vec{N} \cdot \vec{n} = \sin(\theta + u) \sin^2\phi \tag{25}$$

A quadruple integral that expresses the efficiency is calculates as follows but only these parameters, where $\vec{N} \cdot \vec{n} > 0$:

$$\frac{1}{2\pi} \iint_S \iint_r \vec{N} \cdot \vec{n}\, d\vec{r} \cdot d\vec{S} = \frac{1}{2\pi} \int_{-1}^{0} \int_{\frac{-\pi}{2}}^{\frac{3\pi}{2}} \int_0^{2\pi} \int_{1.415}^{\frac{\pi}{2}} \sin(\theta + u) \sin^2\phi \; d\phi\, d\theta\, du\, dv = 0.307 \tag{26}$$

3.4 Conical Panel

The surface of the conical panel, with radius a and height 1 is parametrized by the equation $\vec{r}(u,v) = \langle av \sin u\,, av\cos u\,, -v\rangle$. The range of parameters is $u \in \left[\frac{-\pi}{2}, \frac{3\pi}{2}\right]$ and $v \in [-1,0]$. The variable a represents a real

parameter which is the radius of the base. The area of such a cone is $a\pi\sqrt{1+a^2}$. Then the tangent vectors are

$$\frac{\partial \vec{r}}{\partial u} = \langle av\cos u\,, -av\sin u\,, 0\rangle \text{ and } \frac{\partial \vec{r}}{\partial v} = \langle a\sin u\,, a\cos u\,, -1\rangle \tag{27}$$

With the normal vector

$$\vec{n} = \frac{\partial \vec{r}}{\partial u} \times \frac{\partial \vec{r}}{\partial v} = av\langle \sin u\,, \cos u\,, a\rangle \tag{28}$$

The dot product of $\vec{N}$ and $\vec{n}$ is

$$\vec{N} \cdot \vec{n} = \langle \cos\theta \sin^2\phi\,, \sin\theta \sin^2\phi\,, \cos\phi \sin\phi\rangle \cdot av\langle \sin u\,, \cos u, a\rangle =$$
$$= av(\cos\theta \sin u \sin^2\phi + \sin\theta \cos u \sin^2\phi + a\cos\phi \sin\phi) = av\sin^2\phi\,(\sin(\theta+u) + a\cot\phi) \tag{29}$$

A quadruple integral that expresses the efficiency is calculates as follows but only these parameters, where $\vec{N}\cdot\vec{n} > 0$:

$$\frac{1}{a\pi\sqrt{1+a^2}} \iint_S \iint_r \vec{N}\cdot\vec{n}\, d\vec{r}\cdot d\vec{S} = \frac{1}{a\pi\sqrt{1+a^2}} \int_{-1}^{0} \int_{\frac{-\pi}{2}}^{\frac{3\pi}{2}} \int_{0}^{2\pi} \int_{1.415}^{\frac{\pi}{2}} av\sin^2\phi\,(\sin(\theta+u) + a\cot\phi)\; d\phi\, d\theta\, du\, dv \tag{30}$$

The results of the integration for some values of parameter *a* are displayed in Table 1:

Table 1. Efficiency as a function of the radius of the base

Conical Panel	**Efficiency**
$a = 0.1$	0.3093
$a = 0.15$	0.3097
$a = 0.2$	0.3086
$a = 0.25$	0.3071
$a = 0.3$	0.3051

3.5 Spherical Segment

The surface of the segment of a spherical panel, with radius 1 is parameterized as

$$\vec{r}(u,v) = \langle \cos u \sin v\,, \sin u \sin v\,, \cos v\rangle \tag{31}$$

With the range of parameters $u \in \left[\frac{-\pi}{2}, \frac{3\pi}{2}\right]$ and $v \in \left[b, \frac{\pi}{2}\right]$. Here the parameter *b* denotes the trim of the cup and ranges from 0 to $\frac{\pi}{2}$. Then the tangent vectors are

$$\frac{\partial \vec{s}}{\partial u} = \langle -\sin u \sin v\,, \cos u \sin v\,, 0\rangle \text{ and } \frac{\partial \vec{s}}{\partial v} = \langle \cos u \cos v\,, \sin u \cos v\,, -\sin v\rangle \tag{32}$$

With the normal vector

$$\vec{n} = \frac{\partial \vec{s}}{\partial u} \times \frac{\partial \vec{s}}{\partial v} = \langle \cos u \sin^2 v\,, \sin u \sin^2 v\,, \cos v \sin v\rangle. \tag{33}$$

The dot product of $\vec{N}$ and $\vec{n}$ is

$$\vec{N} \cdot \vec{n} = \langle \cos\theta \sin^2\phi\,, \sin\theta \sin^2\phi\,, \cos\phi \sin\phi \rangle \cdot \langle \cos u \sin^2 v\,, \sin u \sin^2 v\,, \cos v \sin v \rangle \quad (34)$$

Which simplifies to

$$\vec{N} \cdot \vec{n} = \sin^2\phi \sin^2 v\,(\cos(\theta - u) + \cot\phi \cot v) \quad (35)$$

A quadruple integral that expresses the etendue is calculates as follows but only these parameters, where $\vec{N} \cdot \vec{n} > 0$:

$$\iint_S \iint_r \vec{N} \cdot \vec{n}\, d\vec{r} \cdot d\vec{S} = \int_b^{\frac{\pi}{2}} \int_{\frac{-\pi}{2}}^{\frac{3\pi}{2}} \int_0^{2\pi} \int_{1.415}^{\frac{\pi}{2}} \sin^2\phi \sin^2 v\,(\cos(\theta - u) + \cot\phi \cot v)\; d\phi\, d\theta\, du\, dv \quad (36)$$

The results of the integration for some values of parameter b are displayed in Table 2:

Table 2. Efficiency as a function of a trim

Spherical Segment	Efficiency
$b = 0.7$	0.2483
$b = 0.8$	0.2979
$b = 0.9$	0.3572
$b = 1$	0.4318

4. CALCULATIONS FOR PANELS AT THE EQUATOR

As mentioned before, the surface of the spherical segment of the light source is parameterized by the following equation:

$$\vec{S}(\theta, \phi) = \langle \cos\theta \sin\phi\,, \sin\theta \sin\phi\,, \cos\phi \rangle \quad (37)$$

with the range of the parameters: $\theta \in [-\frac{\pi}{2}, \frac{\pi}{2}]$ and $\phi \in \left[\frac{\pi}{2} - 0.15, \frac{\pi}{2} + 0.15\right] = [1.415, 1.721]$. The normal vector is

$$\vec{N} = \langle \cos\theta \sin^2\phi\,, \sin\theta \sin^2\phi\,, \cos\phi \sin\phi \rangle. \quad (38)$$

The coordinate system is in this model is chosen the same way as in the previous model, described for example in [3].

4.1 Horizontal Panel

The surface of the flat horizontal panel located on the equator is parametrized by the equation $\vec{r}(y, z) = \langle 0, y, z \rangle$, with the range of the parameters $y \in [0,1]$ and $z \in [0,1]$. Its area is equal to 1. Then the tangent vectors are

$$\frac{\partial \vec{r}}{\partial z} = \langle 0,0,1 \rangle \text{ and } \frac{\partial \vec{r}}{\partial y} = \langle 0,1,0 \rangle \quad (39)$$

And the normal vector is

$$\vec{n} = \frac{\partial \vec{r}}{\partial z} \times \frac{\partial \vec{r}}{\partial y} = \langle 1,0,0 \rangle \quad (40)$$

The dot product of $\vec{N}$ and $\vec{n}$ is

$$\vec{N} \cdot \vec{n} = \langle \cos\theta \sin^2\phi\,, \sin\theta \sin^2\phi\,, \cos\phi \sin\phi \rangle \cdot \langle 1,0,0 \rangle = \cos\theta \sin^2\phi \quad (41)$$

A quadruple integral that expresses the etendue is calculates as follows but only these parameters, where $\vec{N} \cdot \vec{n} > 0$:

$$\iint_S \iint_r \vec{N} \cdot \vec{n}\, d\vec{r} \cdot d\vec{S} = \int_0^1 \int_0^1 \int_{-\frac{\pi}{2}}^{\frac{\pi}{2}} \int_{1.415}^{1.721} \cos\theta \sin^2\phi \; d\phi \, d\theta \, dx \, dy = 0.6143 \tag{42}$$

4.2 Cylindrical Segment

The surface of a cylindrical segment, with radius 1 and height 1 is parametrized by the equation $\vec{r}(u,v) = \langle \sin u, \cos u, -v \rangle$. The range of parameters is $u \in [c, \pi - c]$ and $v \in [-1,0]$. The optimization is taken with respect to the parameter c that ranges between 0 and $\frac{\pi}{2}$. The are of such a segment is $\pi - 2c$. The tangent vectors are

$$\frac{\partial \vec{r}}{\partial u} = \langle \cos u, -\sin u, 0 \rangle \text{ and } \frac{\partial \vec{r}}{\partial v} = \langle 0,0,-1 \rangle \tag{43}$$

With the normal vector

$$\vec{n} = \frac{\partial \vec{r}}{\partial u} \times \frac{\partial \vec{r}}{\partial v} = \langle \sin u, \cos u\, 0 \rangle \tag{44}$$

The dot product of $\vec{N}$ and $\vec{n}$ is

$$\vec{N} \cdot \vec{n} = \langle \cos\theta \sin^2\phi, \sin\theta \sin^2\phi, \cos\phi \sin\phi \rangle \cdot \langle \sin u, \cos u, 0 \rangle = \cos\theta \sin u \sin^2\phi + \sin\theta \cos u \sin^2\phi \tag{45}$$

which simplifies to

$$\vec{N} \cdot \vec{n} = \sin(\theta + u) \sin^2\phi \tag{46}$$

A quadruple integral that expresses the efficiency is calculates as follows but only these parameters, where $\vec{N} \cdot \vec{n} > 0$:

$$\frac{1}{\pi - 2c} \iint_S \iint_r \vec{N} \cdot \vec{n}\, d\vec{r} \cdot d\vec{S} = \frac{1}{\pi - 2c} \int_{-1}^{0} \int_{c}^{\pi - c} \int_{-\frac{\pi}{2}}^{\frac{\pi}{2}} \int_{1.415}^{1.721} \sin(\theta + u) \sin^2\phi \; d\phi \, d\theta \, du \, dv \tag{47}$$

The results of the integration for some values of parameter *c* are displayed in Table 3:

Table 3. Efficiency as a function of a trim

Cylindrical Segment	Efficiency
$c = 1.25$	0.6117
$c = 1.35$	0.61308
$c = 1.45$	0.61395
$c = 1.55$	0.61431

4.3 Spherical Segment

The surface of a spherical segment, with radius 1 is parameterized by

$$\vec{r}(u,v) = \langle \cos u \sin v, \sin u \sin v, \cos v \rangle \tag{48}$$

With the range of parameters $u \in \left[\frac{-\pi}{2} + d, \frac{\pi}{2} - d\right]$ and $v \in \left[\frac{\pi}{2} - 0.15, \frac{\pi}{2} + 0.15\right]$. Here the parameter *d* denotes the trim of the parameter *u* which determines the length of the spherical stripe and ranges from 0 to $\frac{\pi}{2}$. The area of such a spherical segment is approximately $A = 0.97 - 0.62c$. The tangent vectors are

$$\frac{\partial \vec{s}}{\partial u} = \langle -\sin u \sin v\,, \cos u \sin v\,, 0\rangle \text{ and } \frac{\partial \vec{s}}{\partial v} = \langle \cos u \cos v\,, \sin u \cos v\,, -\sin v\rangle \quad (49)$$

With the normal vector

$$\vec{n} = \frac{\partial \vec{s}}{\partial u} \times \frac{\partial \vec{s}}{\partial v} = \langle \cos u \sin^2 v\,, \sin u \sin^2 v\,, \cos v \sin v\rangle. \quad (50)$$

The dot product of $\vec{N}$ and $\vec{n}$ is

$$\vec{N} \cdot \vec{n} = \langle \cos\theta \sin^2\phi\,, \sin\theta \sin^2\phi\,, \cos\phi \sin\phi\rangle \cdot \langle \cos u \sin^2 v\,, \sin u \sin^2 v\,, \cos v \sin v\rangle \quad (51)$$

Which simplifies to

$$\vec{N} \cdot \vec{n} = \sin^2\phi \sin^2 v\,(\cos(\theta - u) + \cot\phi \cot v) \quad (52)$$

A quadruple integral that expresses the etendue is calculates as follows but only these parameters, where $\vec{N} \cdot \vec{n} > 0$:

$$\frac{1}{A}\iint_S \iint_r \vec{N} \cdot \vec{n}\, d\vec{r} \cdot d\vec{S} = \frac{1}{A}\int_{1.415}^{1.721} \int_{\frac{-\pi}{2}+d}^{\frac{\pi}{2}-d} \int_{\frac{-\pi}{2}}^{\frac{\pi}{2}} \int_{1.415}^{1.721} \sin^2\phi \sin^2 v\,(\cos(\theta - u) + \cot\phi \cot v)\; d\phi\, d\theta\, du\, dv \quad (53)$$

The results of the integration for some values of parameter *d* are displayed in Table 4:

Table 4. Efficiency as a function of a parameter *d*

Spherical Segment	**Efficiency**
$d = 1.35$	0.6094
$d = 1.4$	0.61
$d = 1.45$	0.6111
$d = 1.5$	0.612
$d = 1.55$	0.612

5. SUMMARY OF THE RESULTS AND FUTURE WORK

All numerical results are summarized in Table5 below.

Table 5. Efficiency of analyzed shapes

Shape	**Location**	**Efficiency**
Horizontal panel	North Pole	0.0747
Vertical panel	North Pole	0.307
Cylindrical panel	North Pole	0.307
Conical panel	North Pole	0.3097 with $a = 0.15$
Spherical segment	North Pole	0.4318 with $b = 1$
Horizontal Panel	Equator	0.6143
Cylindrical segment	Equator	0.61431 with $c = 1.55$
Spherical Segment	Equator	0.612 with $d = 1.5$

Among the analyzed shapes the most efficient on the North Pole is a spherical segment with the value of the parameter $b = 1$. However, according to the model, the panels located at the Equator are more efficient that these at the North Pole. The most efficient location is the Equator then with the horizontal panel or cylindrical panel with parameter $c = 1.55$.

So far, we analyzed five shapes on the North Pole and three shapes on the Equator. For the future research we consider analyzing more shapes at other locations. Another option for future work is to describe the position of the sun and the distribution of luminosity on the sky segment that represents the light source in the etendue.

ACKNOWLEDGEMENTS

This research is a result of a collaborative effort among NASA interns and STEM students of LaGuardia Community College and the College of Staten Island. Without the support of NASA Goddard Space Flight Center and specifically Matthew Pearce, this project would not be possible. The guidance, instruction, and patience of Dr. Marciniak was instrumental in the completion of this project. A heartfelt thanks to Dr. Hassebo for fostering this research opportunity and providing the financial means necessary. Peer mentors such as Delfino Enriquez-Torres were wonderful sources of guidance and mathematical support. Special thanks to Rosalba Giarratano of NASA GISS for her day in and day out work. The research was partially supported by the PSC CUNY grant no 61802-00 49 and by CUNY Research Scholars Program.

REFERENCES

[1] Dove, A., Robbins, S., & Wallace, C. (2005, September). The Lunar Orbit Throughout Time and Space. Retrieved on July 1 2019,from http://citeseerx.ist.psu.edu/viewdoc/download;jsessionid=37BC1C762373725B0B8B0E89E1715D2F?doi=10.1.1.371.6408&rep=rep1&type=pdf.

[2] Fitzpatrick, R. (2010, July 21). The Moon. Retrieved on July 1 2019, from http://farside.ph.utexas.edu/books/Syntaxis/Almagest/node38.html.

[3] Marciniak M., Hassebo Y., E.-T. D. S.-R. M., "Efficiency of geometric designs of flexible solar panels: Mathematical simulation," in [Nonimaging Optics: Efficient Design for Illumination and Solar Concentration XIV], Proc. SPIE 10379 (2017).

[4] Marciniak M., Hassebo Y., E.-T. D., K. R., M. E., P., N. "Efficient geometry of flexible solar panels optimized for the latitude of New York City" SPIE Proceedings Volume 10758, [Nonimaging Optics: Efficient Design for Illumination and Solar Concentration XV], 2018

[5] Pandya R., Raja H., E.-T. D. S.-R. M. H. Y. M. M., "Mathematical simulation of efficiency of various shapes of solar panels for NASA geostationary satellites," in [Physics, Simulation and Photonics Engineering of Photovoltaic Devices VII], Proc. SPIE 10527 (2018).

[6] Roncoli, R. B. (2005, September 23). Lunar Constants and Models Document. Retrieved July 1, 2019 from https://www.hq.nasa.gov/alsj/lunar_cmd_2005_jpl_d32296.pdf.

[7] Stewart, J. (2016, September). Single Variable Calculus: Early Transcendentals. Eight edition. Retrieved July 1, 2019, from https://www.cengage.com/c/calculus-early-transcendentals-8e-stewart/9781285741550PF/.

[8] Tabor, A. (2018, August 21). Ice Confirmed at the Moon's Poles. Retrieved on September 1, 2019 from https://www.nasa.gov/feature/ames/ice-confirmed-at-the-moon-s-poles.

[9] Williams, D. (2019, April 22). Earth Fact Sheet. Retrieved on July 1, 2019 from https://nssdc.gsfc.nasa.gov/planetary/factsheet/earthfact.html.